

# AIRFRAME NOISE MEASUREMENTS BY USING A SIMPLIFIED HIGH-LIFT MODEL

Hiroki Ura\*, Yuzuru Yokokawa\*, Taro Imamura\*, Takeshi Ito\*, Kazuomi Yamamoto\*  
\*Japan Aerospace Exploration Agency

**Keywords:** *Airframe Noise, New Test Section, High Lift Devices, Phased Array Microphone*

## Abstract

*This paper describes high-lift device noise measurements at four types of test section in three different wind tunnels. Those are a new anechoic test section and a hard-wall test section in Japan Aerospace Exploration Agency (JAXA), an open-jet test section in Railway Technical Research Institute (RTRI), and an anechoic test section in Virginia Tech.*

*By comparing the results in these wind tunnels, the capability of aeroacoustic measurement in the JAXA new anechoic test section is investigated. Although there are several small differences between the new test section data and the others, the results show the reduction of sidelobe, good agreement of not only total noise spectrum but also each noise component with in open-jet anechoic test section. Therefore, the advantage for aeroacoustic measurement in JAXA LWT2 anechoic test section is shown compared with the aeroacoustic measurement in LWT2 hard wall test section.*

## 1 Introduction

Airframe noise from high-lift-devices (HLD) and landing gears is contributing as a principal factor for the overall noise level during approach and landing phase due to reduction of the engine noise in recent years. Many studies for clarification of generation mechanism and reduction of airframe noise around HLD and landing gear have been carried out from both experimental and computational aspects until now [1]-[3]. It is difficult to apply proposed noise reduction concepts to actual aircraft and to reduce airframe noise in actual flight because of some reasons such as complex geometry of

actual aircraft, complex flow field, Reynolds number effect and so on. In particular, design of quiet HLD requires achieving not only aeroacoustic high performance but also aerodynamic high performance.

In JAXA, research for airframe noise from HLD has been started to obtain their design approach to achieve both low noise and aerodynamic high performance. To reduce airframe noise from HLD, basic characteristics have to be understood in detail. As a first step for our research of airframe noise, aeroacoustic and aerodynamic measurements were conducted by using simplified three-element wing model to investigate relationship between airframe noise and the phenomena of flow field around HLD. The aerodynamic measurements and the phased array microphone measurements were carried out in hard-wall test section at JAXA 2 m by 2 m Low-speed Wind Tunnel (LWT2). The far-field noise measurements and the phased array microphone measurements were also conducted in open-jet test section at RTRI Large-Scale Anechoic Wind Tunnel in Japan [4]-[9]. However, the wind tunnel testing under the high-lift flow condition is restricted in open-jet test section because the jet flow cannot be collected under the high-lift condition by jet-catcher and the flow becomes unstable. A new concept of test section, which has characteristics of aerodynamically closed and acoustically open test section, was proposed by Virginia Tech to deal with such problems [10]-[12]. The unique and innovative concept has been applied to the Virginia Tech anechoic wind tunnel (VT). To evaluate capability of this test section, aerodynamic and aeroacoustic testing was carried out by using the JAXA's simplified HLD wing model in 2007. Its advantage in

acoustic measurements over conventional test section and favorable aerodynamic characteristics were shown through the comparison with data from a hard-wall test section in JAXA LWT2 and an open-jet test section in RTRI [13].

This concept was also applied to the test section at JAXA LWT2 in 2008. First aerodynamic and acoustic measurements were conducted in a JAXA's new test section by using same HLD model, and the test section was evaluated and validated by comparing to test results in VT anechoic test section [14].

In addition, the basic characteristics of the high-lift model were shown in our previous studies [4]-[8], [13]. The points of the acoustic characteristics are shown in the follows. The slat noise is dominant at lower frequency below 2 kHz and higher frequency above 10 kHz. The lower frequency noise is generated near the shear-layer reattachment region at the slat cove, and has several peaks of frequency. The slat noise at higher frequency is caused by Karman vortices at the trailing-edge of the slat. As AoA changes, these slat noise level and frequency change. Similarly, the static pressure at the slat change with AoA. On the other hand, the flap noise is clearly observed at frequency between 2 kHz to 10 kHz. Unlike slat noise, its static pressure distribution at the flap does not depend on AoA. This is well known as one of the aerodynamic characteristics of flap, and it is due to remaining of the same location of the vortex generated by the flap side edge.

In this paper, the capability for airframe noise measurements in a new test section at JAXA LWT2 is evaluated in more detail through the comparison with data from the new test section in JAXA LWT2 and in the others by using the same model.

## 2 Simplified High Lift Model

Fig.1 shows the simplified high lift wing model which was designed to research high-lift device noise. This model has 0.6 m in the chord length, 1.40 m in the half span, no sweep angle, no taper and no dihedral angle. The model consists of three simplified wing elements and body pod. The HLD are full-span slat at the leading-edge

and 70 % span single-slotted flap at trailing-edge, which are supported by four tracks. The deflection angles of slat and flap are 25 degrees and 35 degrees, respectively. In addition, a simplified body pod with 1.65 m length and 0.4 m width formed by ellipse cross sections is also equipped. Reynolds Number based on the chord length is up to about 2.3 million ( $U=60$  m/s) in this series of wind tunnel testing.

The model has 189 static pressure taps at four sections across slat, main wing and flap as shown in Fig. 2. The measurements of surface pressure were carried out by using electric scanning pressure system in LWT2 and by using mechanical scanivalve system in the other wind tunnels. In order to evaluate aeroacoustic data under the same condition of flow field around the test model, these static pressure distribution data was taken.

Two model configurations were mainly used in this series of experiment using this model. One of them is "landing configuration" where both the slat and the flap are deployed, and the other is "slat deployed configuration" where the slat is only deployed and the flap is stowed.



Fig. 1 Simplified High-Lift Model

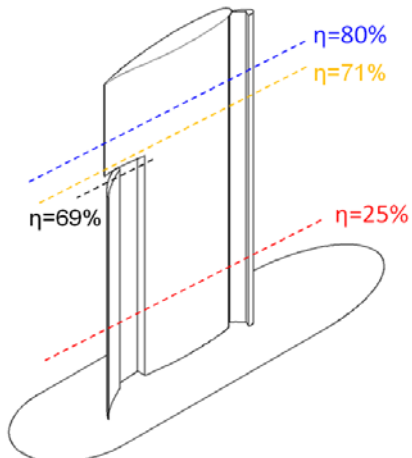


Fig. 2 Span wise locations for static pressure taps

### 3 Wind Tunnels and Experimental Setup

The series of this work were carried out in four types of test section in three wind tunnels. In general, there is a difference of the flow field around the test model between in hard wall test section and in open-jet test section because of difference of wall interference. Similarly, the test section with Kevlar wall should have wall interference more or less, because Kevlar wall is a kind of porous material wall. In JAXA, six component aerodynamic data are usually corrected by a conventional boundary correction, and the correction was applied to the aerodynamic data which was obtained at LWT2. Unfortunately, the aerodynamic measurements by using force balance at RTRI and VT could not be conducted because of capacity shortage of force balance. Hence, these wall interferences were investigated by using surface pressure data which were measured at all wind tunnels.

#### 3-1 JAXA LWT2

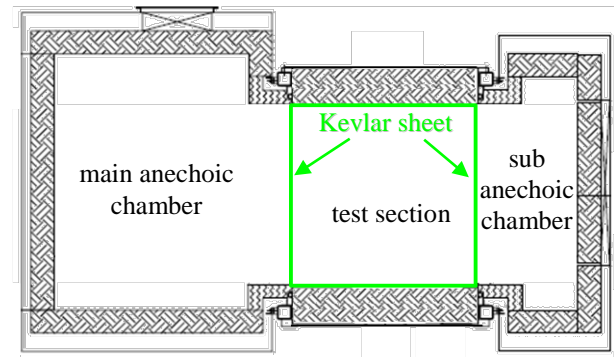
LWT2 is an atmospheric pressure closed circuit type and conventional wind tunnel. LWT2 has two types of test section, a hard-wall rectangular test section (LWT2\_H) as shown in Fig. 3 and an anechoic test section with anechoic chambers (LWT2\_A) as shown in Fig. 4. With regard to the anechoic test section, the tensioned Kevlar sheets are installed at the boundary of each anechoic chamber and test section. The test section also has anechoic ceiling and floor with porous metal sheets covered with Kevlar sheets with acoustic absorber. The test section has a main anechoic chamber on the one side and a sub anechoic chamber on the other side. Acoustic characteristics of the main chamber had been confirmed by evaluation based on ISO/DIS 3745.

The aerodynamic measurements have been done for aerodynamic force, static pressure, PIV and oilflow visualization using hard wall test section at LWT2. Here, the measurement using force balance was conducted only in LWT2. The reason is that this force balance cannot be set in the other wind tunnels due to too larger size of the balance. On the other hand, the static pressure of the model was also measured in the other wind tunnels. Thus, the pressure

distributions are available to evaluate these acoustic data under the same condition of flow field.



Fig. 3 JAXA LWT2 hard wall test section



(a) Cross sectional view of test section with anechoic chambers



(b) Anechoic chamber (c) Test section

Fig. 4 JAXA LWT2 anechoic test section

Acoustic data was acquired by phased array microphone system in both test section at LWT2. The arrays consist of 48 microphones in the hard wall test section and 96 microphones in the anechoic test section, respectively. The microphone is B&K type 4958 which has diameter of 7 mm, the frequency range of 10 Hz to 20 kHz and the dynamic range of 30 dB to 140 dB. The array for hard wall test section was

mounted on the side wall of the test section, and the array for anechoic test section was set in the main anechoic chamber. These arrays are multi-arm shaped, and their diameters are 1 m and 1.5 m, respectively. Acquisition noise data was processed by frequency domain conventional beamforming method. Calculating area of sound pressure level was 1500 mm x 1500 mm and was set on the lower surface of test model. The contour range of acoustic map is 7 dB.

### 3-2 RTRI anechoic wind tunnel

RTRI is an atmospheric pressure closed circuit type wind tunnel, which has cross-section of 3.0 m in width and 2.5 m in height and 8 m long open test section as shown in Fig. 5. In addition, it is the most remarkable feature of this wind tunnel that the background noise level is under 75.6 dB (A) at 300 km/h at the test section [9].

1/4 inch diameter non-directional condenser microphone (B&K type 4939) which has the frequency range up to 100 kHz was used for the far-field noise measurements in this wind tunnel. The microphone was located at 1.5 times of width of the test section (4.5 m) away from lower side of the model in order to reduce the effect of shear from nozzle, and set on the same plane where the model was supported to reduce the reflection of airframe noise at the lower floor. The far-field noise data by condenser microphone is used as the reference noise data in order to compare with phased array data in this paper.

The phased array measurements were also done in this tunnel. The arrays of 1 m diameter and 4 m diameter were used at RTRI testing. These microphone arrays which are B&K “wheel array” have similarity shape and consist of 66 microphones. The array data was obtained by B&K PULSE system and was reduced by JAXA in-house beamforming code to eliminate characteristic variation caused by different post-process code.

### 3-3 VT anechoic wind tunnel

The Virginia Tech Stability Wind Tunnel is a continuous, single return, subsonic wind tunnel with a 7.3-m long removable test section, with a square cross section 1.83 m on edge. The wind tunnel achieves a maximum speed in the test

section of about 80 m/s for a Reynolds number per meter up to about 5.3 million. Virginia Tech designed a unique anechoic test section to convert it to anechoic wind tunnel [10]. The new concept involved the construction and installation of a test section with walls formed largely from tensioned Kevlar cloth embedded in an anechoic chamber as shown in Fig. 6.

Phase array data was collected using 66 microphones. This array is star shaped, and consists of 7 arms with 9 microphones per arm. The array was set at the anechoic chamber on the pressure side of the model. Acoustic maps were visualized by using JAXA in-house code for the above reason.

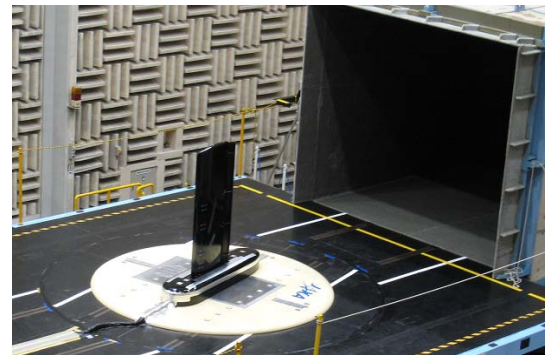
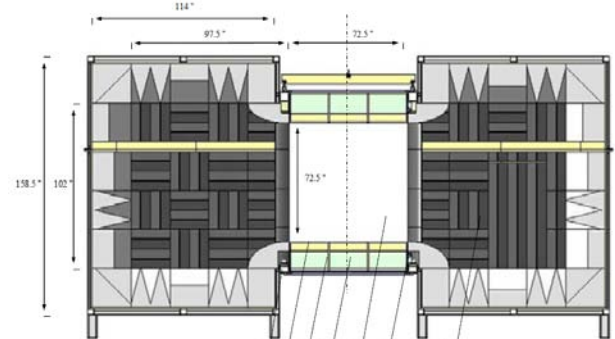
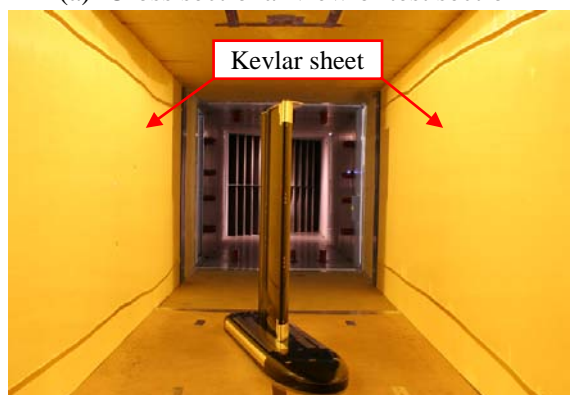


Fig. 5 RTRI large-scale anechoic wind tunnel



(a) Cross sectional view of test section



(b) Test section

Fig. 6 Virginia Tech anechoic tunnel

## 4 Results and Discussions

### 4-1 Condition for Comparison

It is important to compare the total HLD noise at the same local flow condition. Because the HLD noise is related to flow condition such as the location of local flow separation and reattachment and vortices as mentioned above. To evaluate acoustic data, the same conditions of local flow field around test model are investigated by comparing static pressure distributions in each test sections in this section.

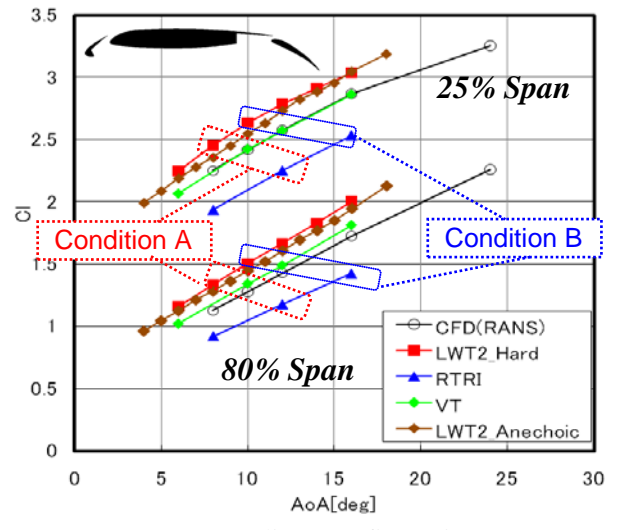
At first, the local lift coefficients are compared by integrating static pressure distribution at 25 % and 80 % span wise sections in order to investigate the equal condition. Fig. 7 shows the comparison of the local lift coefficients. CFD results, which were calculated under free-air condition by using Reynolds-averaged Navier-Stokes equations, are also shown in Fig. 7 as a reference. The lift coefficient of CFD checked with data corrected for wall interference acquired at LWT2 hard wall test section (LWT2\_H) in our previous study. CFD data is useful as a reference for comparing with experimental results for this reason.

Here, these local lift coefficients are affected by wall interference. Compared with CFD data, the data obtained at hard wall test section should be transferred to higher angle of attack and to lower lift coefficient. On the other hand, open test section data should shift in a direction opposite to data of hard wall test section. Next, LWT2 anechoic test section (LWT2\_A) data and VT data have similar characteristic to hard wall data and CFD data, respectively. Therefore, LWT2\_A, which has the tensioned Kevlar sheets, is like hard wall aerodynamically, and the wall interference is smaller than LWT2\_H.

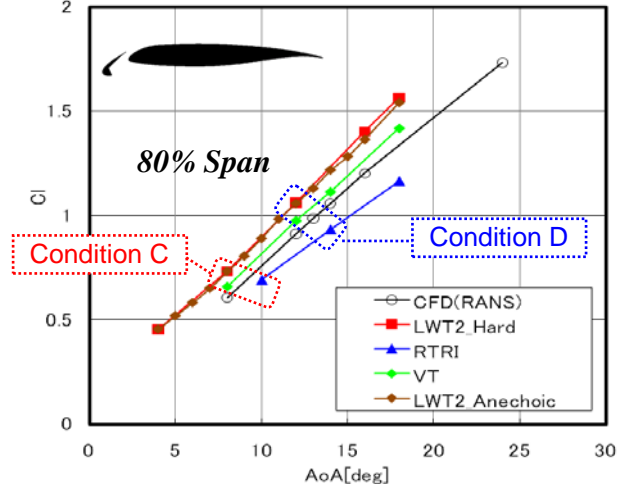
Fig. 8 shows comparison of static pressure distributions at the 25 % span wise section and 69 % span of flap side edge in condition “A”, which have the almost same level of local lift coefficient, as shown in Fig. 7. The static pressures of LWT2\_A at slat region agree with RTRI and LWT2\_H as shown in Fig. 8 (a). There is a difference of the static pressure of VT at the lower side of the slat compared with the others. With regard to main wing and flap, the

static pressure of RTRI on the upper surface is small compared with the others. However, these differences are enough small for acoustic evaluation. In addition, the static pressures of LWT2\_A at the flap side edge show good agreement with the others except for RTRI data as shown in Fig. 8 (b). Although there is a different of static pressure between RTRI and the others at the mid chord of flap, the difference affects too small influence for the characteristics of flap noise. Therefore, the condition “A” is available for the comparison of lower AoA and landing configuration.

Similarly, the each flow fields in condition “B”, “C”, and “D” are almost equivalent, and these conditions are available to compare with acoustic data. The comparisons are conducted in these conditions in the following section.



(a) Landing Configuration



(b) Slat deployed configuration

Fig. 7 Local lift coefficients by integrating static

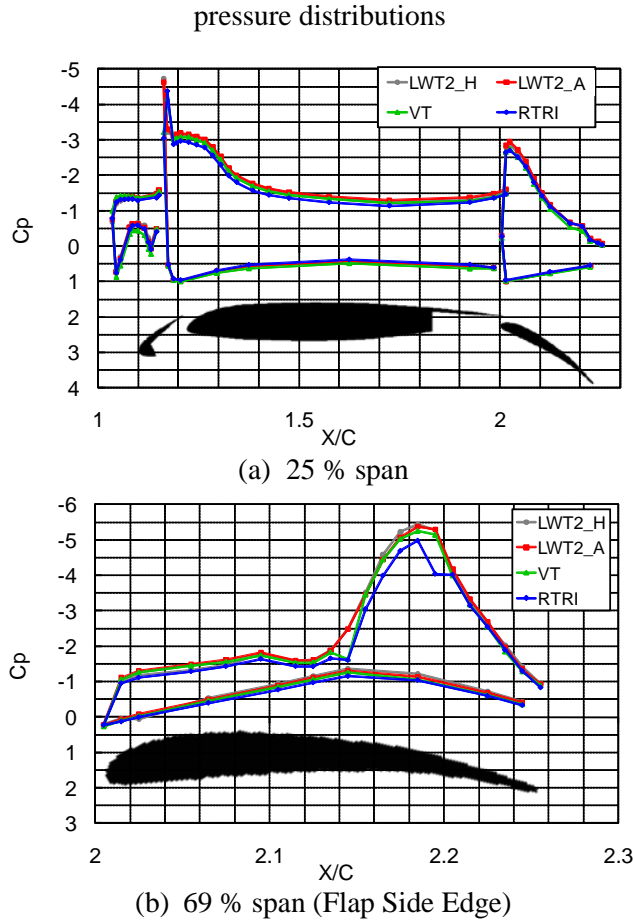


Fig. 8 Static pressure distributions in condition A  
 "LWT2\_A": LWT2 Anechoic test section  
 "LWT2\_H": LWT2 Hard-wall test section

#### 4-2 Acoustic measurements

Fig. 9 shows sound pressure level distribution map in flow condition "A" measured in four test sections at three wind tunnels. The maps show results at center frequency of 2 kHz, 4 kHz, 8 kHz, and 16 kHz in third octave band. The contour range is 7 dB. The results measured at RTRI by using two microphone arrays are shown in Fig. 9 (c) and (d). These arrays have diameter of 4 m and 1 m, respectively.

Noise source are clearly observed at all maps as shown in this figure. Flap side edge noise and slat noise at outboard are dominant noise source at frequency of 2 kHz. Flap noise has relatively higher noise level at frequency of 4 kHz and 8 kHz.

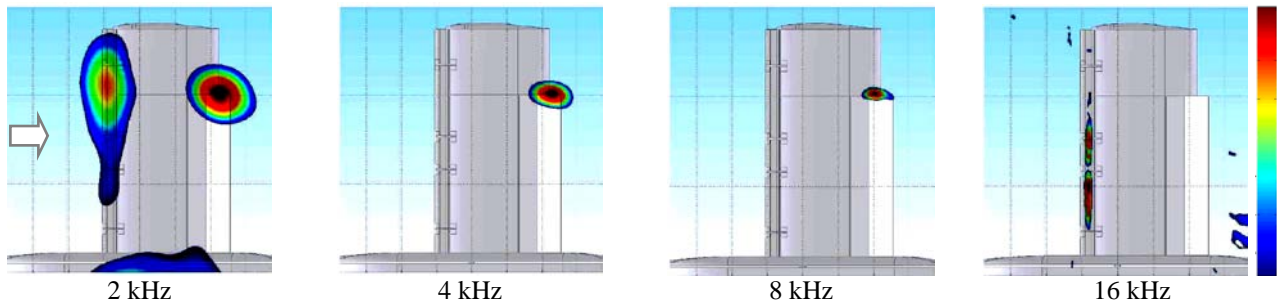
Two-dimensional distribution of sound source on the slat is observed at higher frequency of 16 kHz. The source locations and frequency characteristics of these results are

very good agreement. Spatial resolution among wind tunnels differ significantly, but this is reason why spatial resolution inversely relates for measurement distance and is proportional for array diameter. Here, the phased array measurements were carried out in the conditions of 3 m distance and 1 m array at LWT2\_A. In addition, the measurements were conducted in the conditions of 4.5 m distance and 1 m array, and 4.5 m distance and 4 m array at RTRI open jet test section. The spatial resolution of results at LWT2\_A is 1.5 times spatial resolution by RTRI 4 m array and is about third by RTRI 1 m array. Compared with acoustic map at 4 kHz in Fig. 9 (b), (c) and (d), the above rates of spatial resolution are validated. Therefore, Kevlar wall does not influence the blurring of noise source location. Focusing on the acoustic map at 2 kHz and 16 kHz, the side lobe level of LWT2\_A is less than LWT2\_H because the sound reflection is reduced by acoustic absorvent in the anechoic test section.

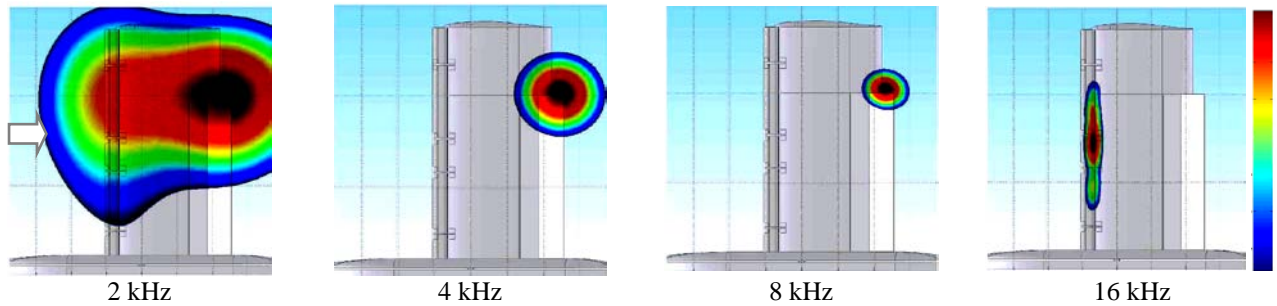
For quantitative comparisons, sound pressure levels are integrated at whole region, slat region and flap region as shown in Fig. 10. Sampling frequencies differ in each wind tunnel testing. In order to validate their frequency characteristics in detail and reduce the effect of frequency resolution, the spectra are evaluated in twelfth octave band. To validate this method, integrated spectrum, which was measured in RTRI by using 1 m array, was compared with far field noise spectrum measured in RTRI by using single condenser microphone as shown in Fig. 11. Ideally, the results should agree completely because these were obtained at the same flow condition. Fig. 11 suggests that the integrated spectrum agrees with far field noise spectrum by single microphone very well. Therefore, acoustic characteristics in each wind tunnel can be quantitatively evaluated by using this method.

Next, it is well known that sound wave is decayed and is refracted by boundary layer in the test section. In addition, the acoustic transmission loss through Kevlar sheet in Kevlar wall test section should be considered for accurate evaluation. In this paper, a simple approach to correct influence is applied as a first step of accurate evaluation.

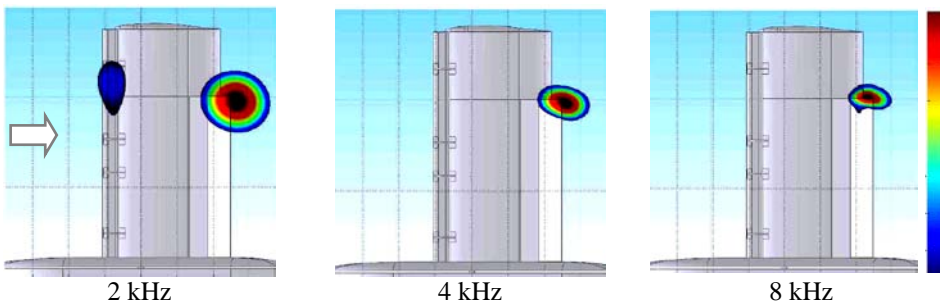
AIRFRAME NOISE MEASUREMENTS BY USING A  
SIMPLIFIED HIGH-LIFT MODEL



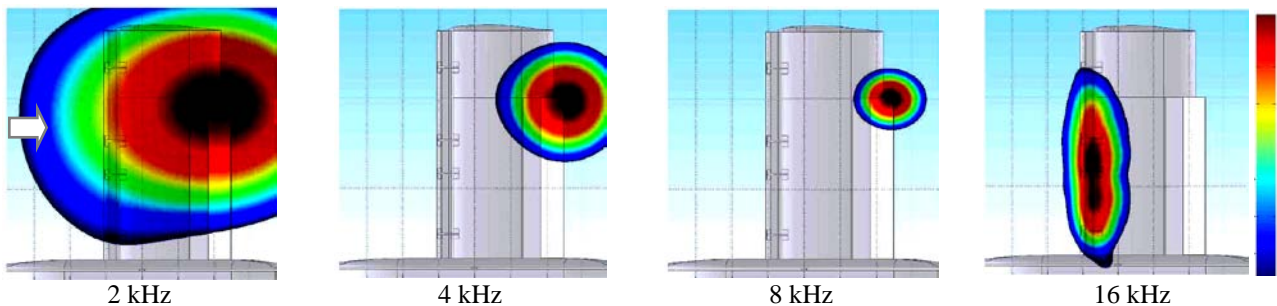
(a) JAXA LWT2 hard-wall test section



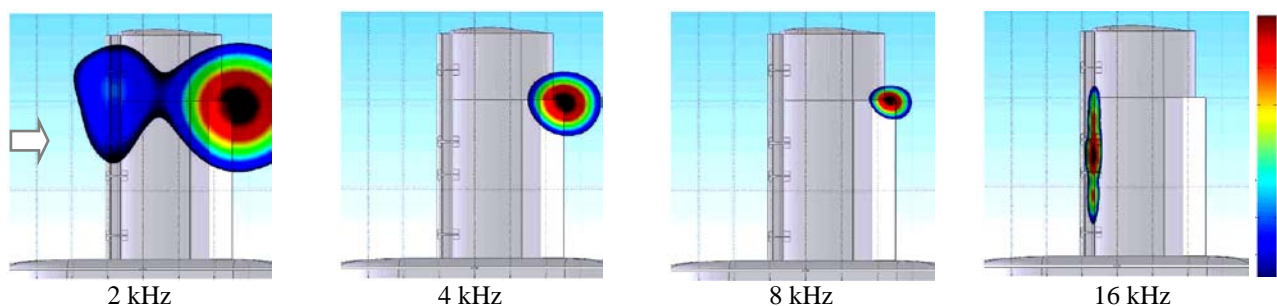
(b) JAXA LWT2 anechoic test section



(c) RTRI open-jet test section (4 m Array)



(d) RTRI open-jet test section (1 m Array)



(e) VT anechoic test section

Fig. 9 SPL distributions in 1/3 octave band for condition A at 50 m/s

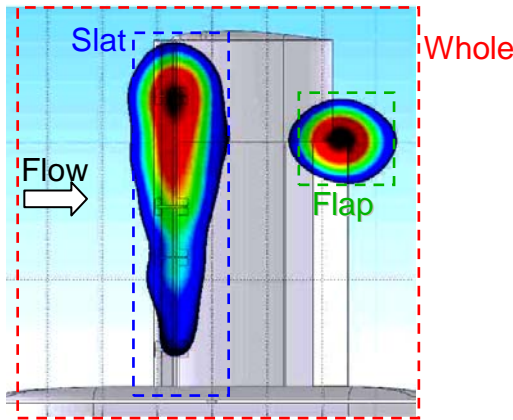


Fig. 10 Region of integration

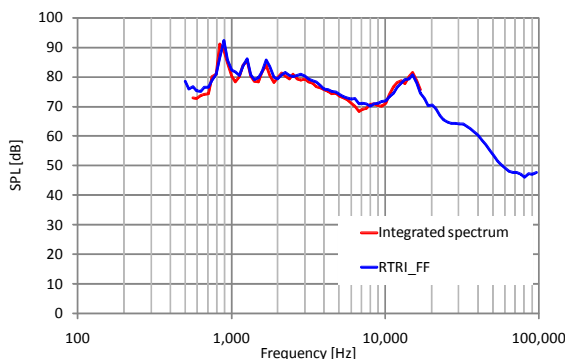
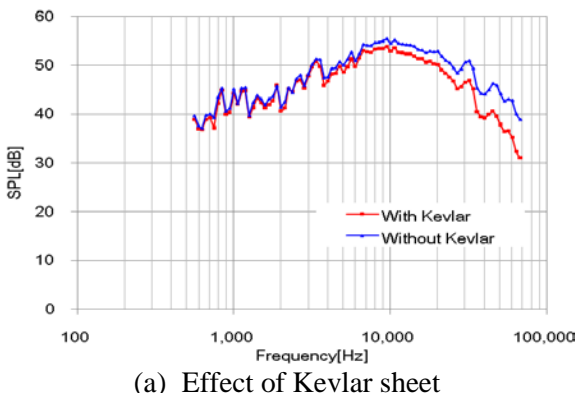
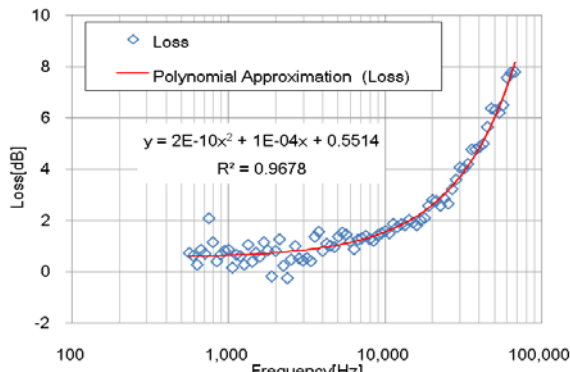


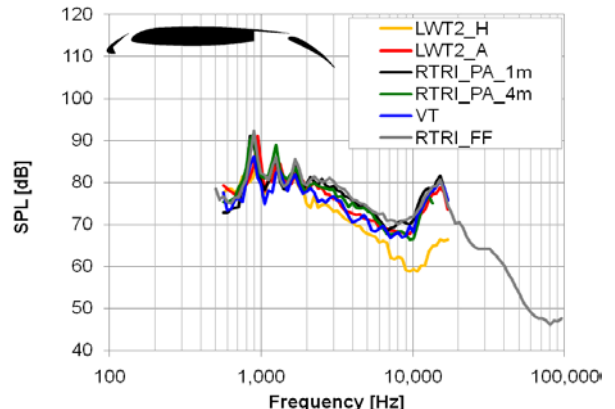
Fig. 11 Comparison of far field noise (RTRI\_FF) measured by a condenser microphone and integrated spectrum



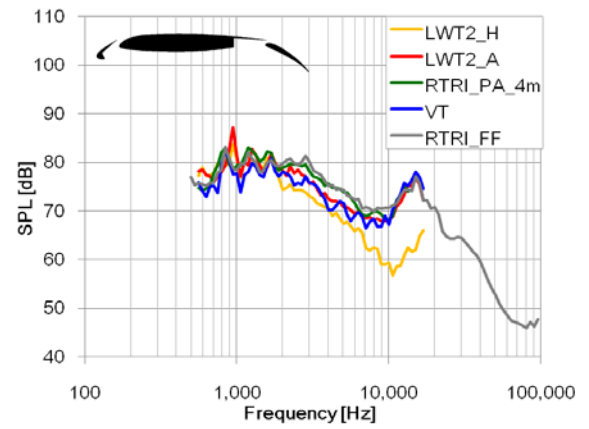
(a) Effect of Kevlar sheet



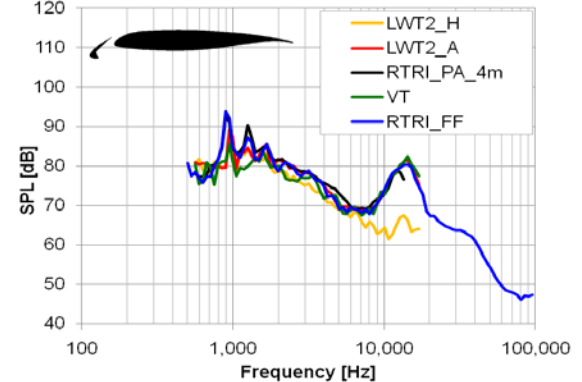
(b) Acoustic loss in 1/12 octave band  
Fig. 12 Acoustic loss through Kevlar sheet



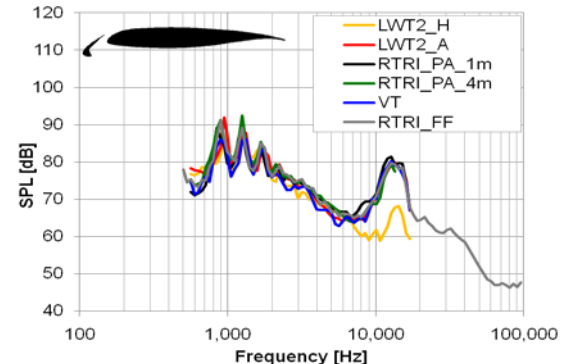
(a) Condition A (lower AoA), landing configuration



(b) Condition B (higher AoA), landing configuration



(c) Condition C (lower AoA), slat configuration



(d) Condition D (higher AoA), slat configuration  
Fig. 13 Comparison of spectra at 50 m/s in 1/12 octave band

Fig. 12 shows measurement result of acoustic loss through Kevlar sheet which was investigated in LWT2\_A by using loudspeaker. The following equation was obtained from this result as a compensation formula for the acoustic loss by Kevlar.

$$\Delta[dB] = 0.0002 \left( \frac{f[Hz]}{1000} \right)^2 + 0.1 \left( \frac{f[Hz]}{1000} \right) + 0.5514$$

This equation is applied to the acoustic data obtained in LWT2\_A. The other acoustic data should be corrected as the data of LWT2\_A. Acoustic measurements in LWT2\_H were conducted by using phased array microphone which was flash mounted on side wall. Thus, 6 dB is deducted from LWT2\_H data as a rough estimation of sound reflection. Measurement results in VT are corrected by the data of acoustic loss and advection loss reported by Remillieux [12]. In addition, the distance decay is corrected as reference distance of 1 m, because measurement distance is different in each wind tunnel. The following shows corrected results.

Fig. 13 shows comparison of far field noise by single condenser microphone and spectra which are integrated over whole region of sound pressure distribution. Fig. 13 (a), (b), (c), and (d) show the results at the condition of lower angle of attack and landing configuration, higher angle of attack and landing configuration, lower angle of attack and slat-deployed configuration, and higher angle of attack and slat-deployed configuration, respectively. In order to check dominant noise source of data in LWT2\_A, the integrated spectra at slat region, flap region and whole region are compared as shown in Fig. 14. The dominant noise sources of this result are peak noise of slat at the frequency below 2 kHz, slat trailing edge noise at the frequency above 10 kHz, and flap noise at the frequency between 2 kHz and 10 kHz, and this result corresponds with the previous studies. Compared to the RTRI data, the level of lower frequency slat noise in LWT2\_A is almost equal to RTRI, but there is a difference of its peak frequency. The spectrum of higher frequency slat noise agrees with RTRI. The level of flap noise in LWT2\_A is about 2 dB smaller than RTRI. This may be caused by the different location of flap-tip vortex between

LWT2\_A and RTRI as shown in Fig. 8 (b). On the other hand, the several buildups of VT data are observed at the frequency between 2 kHz and 10 kHz compared with the other data. The flap noise is dominant at this frequency. However, this phenomenon is also observed in the results of slat configuration as shown in Fig. 8 (c) and (d). Although this remains to be identified yet, this is not caused by change of flap noise. Next, compared with LWT2\_H, the significant difference between spectrum of LWT2\_H and the other test sections is observed at frequency above 7 kHz. Despite the measurements in the same wind tunnel facility, the capability of noise measurement in LWT2\_A is higher than LWT2\_H. On the other hand, there is variation of about  $\pm 1.5$  dB between LWT2\_A and the other except LWT2\_H. Possible causes of this variation are un-correction for acoustic loss by boundary layer or shear layer except VT data and variation of flow condition among test sections.

Next, the each noise component is focused on. There is difference of level between each HLD noise and “whole region” noise at frequency below 2 kHz as shown in Fig. 14. Because spatial resolution at the frequency is too large and noise source distribution is larger than each HLD region as shown in Fig. 10, HLD noise spectra may be under-estimated. In addition, slat noise level is relatively higher than flap noise level. Therefore, slat noise is dominant at the frequency below 2 kHz, and the flap noise at the frequency below 2 kHz is affected by the slat noise which has large spatial resolution. As a result, it is difficult to evaluate the flap noise at the frequency below 2 kHz in this experimental setup. For reduction of influence by slat noise, the spatial resolution has to be improved by using larger size array and/or shorter measurement distance.

Fig. 15 shows comparison of HLD noise spectra obtained in four test sections. Characteristics of LWT2\_H noise spectrum differs compared with the other spectra. The lower frequency slat noise in LWT2\_A is almost equal level of RTRI and has different peak frequency of RTRI as the results of integrated spectra at the whole region. In addition, the higher frequency slat noise in LWT2\_A shows good agreement with RTRI data. There is the

difference of about 2 dB in “whole region” spectrum at the frequency from 2 kHz to 10 kHz between LWT2\_A data and RTRI data as shown in Fig. 13 (a) and (b). However, “slat region” spectrum of LWT2\_A match RTRI data as shown in Fig. 15 (a). Moreover, the buildup of VT data is also observed in this result. Thus, this is not caused by change of flap noise as mentioned above. Next, focusing on flap noise, the LWT2\_A spectrum corresponds with RTRI data at the frequency between 2 kHz and 10 kHz as shown in Fig. 15 (b). On the other hand, the characteristics of each spectrum differ at the frequency above 12 kHz. As shown in Fig. 14, flap noise is about 15 dB smaller than slat noise. The different characteristics may be caused by the performance limit of microphone array because the dynamic range of the microphone array is about 10 dB in the condition of this experimental setup.

## 5 Conclusions

To evaluate the capability of airframe noise measurements in a new anechoic test section at JAXA 2 m x 2 m low-speed wind tunnel, aerodynamic and aeroacoustic measurements were conducted by using a simplified high-lift model as a first step. This new test section has tensioned Kevlar sheets as the side wall of the test section, and the test section is installed with two anechoic chambers. The characteristics of this test section are evaluated and validated through comparison to the results which were measured in VT and RTRI by using the same test model. Although there are several small differences, the results show the reduction of sidelobe, good agreement of not only total noise spectrum but also each noise component with in open-jet anechoic test section. Therefore, the aeroacoustic measurement in JAXA LWT2 anechoic test section is available. In addition, our future work will be to develop more precise acoustic correction.

## Acknowledgements

The authors would like to thank for Dr. Takaishi, Mr. Uda, and other members of RTRI, and Prof. Ng, Prof. Burdisso, and other members

of VT, and Mr. Uchida, Mr. Shimada, and other members of JAXA for their support in this series of wind tunnel experiments.

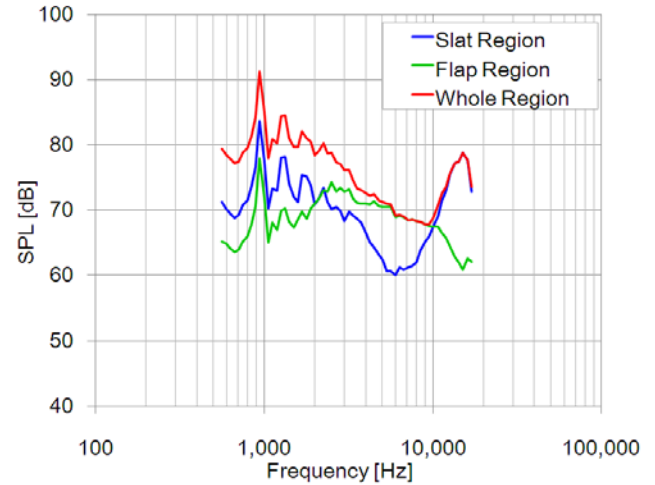


Fig. 14 HLD noise and whole noise

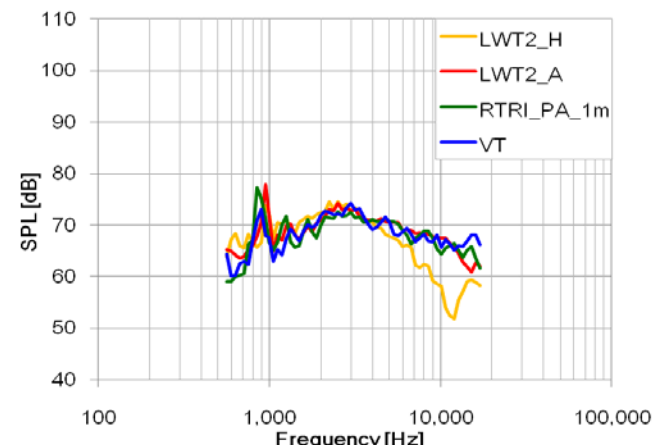
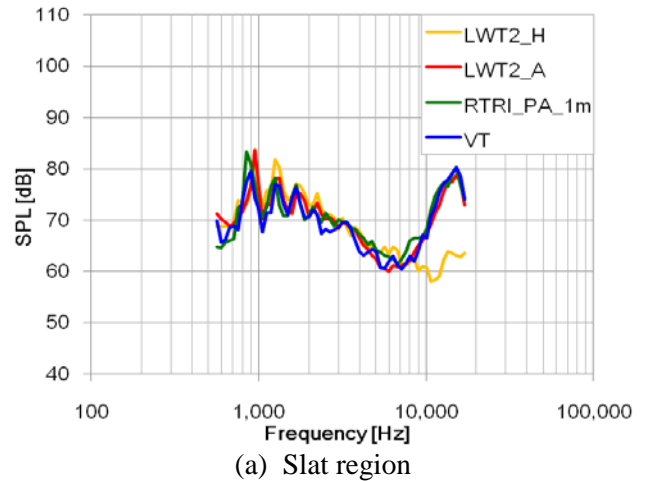


Fig. 15 Comparison of each HLD component

## References

- [1] Chow L.C., Mau K., Remy H., "Landing gears and High Lift Devices Airframe Noise Research", AIAA paper 2002-2408.
- [2] Piet J., Davy R., Elias G., Siller H. A., Chow L. C., Seror C., Laporte F., "Flight Test Investigation of Add-On Treatments to Reduce Aircraft Airframe Noise", AIAA paper 2005-3007.
- [3] Stoker R.W., Underbrink J. R., Neubert G. R., "Investigations of Airframe Noise in Pressurized Wind Tunnels", AIAA paper 2001-2107.
- [4] Yokokawa Y., Ura H., Imamura T., Ito T. and Yamamoto K., "Detail Observation of Noise and Aerodynamics for High-Lift Configuration Model in JAXA", INTER-NOISE 2007.
- [5] Ura H., Yokokawa Y., Imamura T., Ito T. and Yamamoto K., "Investigation of Airframe Noise from High Lift Configuration Model" AIAA paper 2008-0019.
- [6] Imamura T., Ura H., Yokokawa Y., Hirai T., and Yamamoto K., "Numerical and Experimental Research of Low-Noise Slat using Simplified High-lift Model," AIAA paper 2008-2918.
- [7] Yokokawa Y., Imamura T., Ura H., and Yamamoto K., "A Far-field Noise and Near-field Unsteadiness of a Simplified High-lift-configuration Model (Flap-edge)," AIAA paper 2009-283.
- [8] Imamura T., Ura H., Yokokawa Y. and Yamamoto K., "A Far-field Noise and Near-field Unsteadiness of a Simplified High-lift-configuration Model (Slat)," AIAA paper 2009-1239.
- [9] Maeda T., Kondo Y., "RTRI's Large-scale Low-noise Wind Tunnel and Wind Tunnel Tests", Quarterly Report of RTRI, Vol.42, No.2 (2001), pp.65-70.
- [10] Smith B. S., Camargo H. E., Burdisso R. A., and Devenport W. J., "Development and Testing of a Novel Acoustic Wind Tunnel Concept," AIAA paper 2005-3053.
- [11] Remillieux M. C., Camargo H. E., Ravetta P. A., Burdisso R. A. and Ng W. F., "Novel Kevlar-Walled Wind Tunnel for Aeroacoustic Testing of a Landing Gear", AIAA J., Vol.46, No.7, July 2008, pp. 1631-1639
- [12] Remillieux M. C., Crede E. D., Camargo H. E., Burdisso R. A., Devenport W. J., Rasnick M., Seeters P. V., and Chou A., "Calibration and Demonstration of the New Virginia Tech Anechoic Wind Tunnel," AIAA paper 2008-2911.
- [13] Yamamoto K., Ura H., Yokokawa Y., Imamura T., Nakakita K., Camargo H., Remillieux M., Boor Z., Burdisso R. A., Ng W. F., Uchida H., Ito T., "Aeroacoustic Testing of a High-Lift Device Model in the Virginia Tech Anechoic Wind Tunnel", 13<sup>th</sup> CEAS-ASC Workshop & 4<sup>th</sup> Scientific Workshop of X3 – Noise, 2009.
- [14] Ito T., Ura H., Nakakita K., Yokokawa Y., Ng W. F., Burdisso R. A., Iwasaki A., Fujita T., Ando N., Shimada N., Yamamoto K., "Aerodynamic /

Aeroacoustic testing in Anechoic Closed Test Sections of Low-speed wind Tunnels", AIAA paper 2010-3750

## Copyright Statement

The authors confirm that they, and/or their company or organization, hold copyright on all of the original material included in this paper. The authors also confirm that they have obtained permission, from the copyright holder of any third party material included in this paper, to publish it as part of their paper. The authors confirm that they give permission, or have obtained permission from the copyright holder of this paper, for the publication and distribution of this paper as part of the ICAS2010 proceedings or as individual off-prints from the proceedings.